ACS APPLIED MATERIALS & INTERFACES

Research Article

www.acsami.org

Microfluidic Fabrication of Bio-Inspired Microfibers with Controllable Magnetic Spindle-Knots for 3D Assembly and Water Collection

Xiao-Heng He,[†] Wei Wang,[*,†] Ying-Mei Liu,[†] Ming-Yue Jiang,[†] Fang Wu,[†] Ke Deng,[†] Zhuang Liu,[†] Xiao-Jie Ju,[†] Rui Xie,[†] and Liang-Yin Chu[*,†,‡]

[†]School of Chemical Engineering, Sichuan University, No. 24, Southern 1 Section, Yihuan Road, Chengdu, Sichuan 610065, P. R. China

[‡]State Key Laboratory of Polymer Materials Engineering, Sichuan University, Chengdu, Sichuan 610065, P. R. China

Supporting Information

ABSTRACT: A simple and flexible approach is developed for controllable fabrication of spider-silk-like microfibers with tunable magnetic spindle-knots from biocompatible calcium alginate for controlled 3D assembly and water collection. Liquid jet templates with volatile oil drops containing magnetic Fe_3O_4 nanoparticles are generated from microfluidics for fabricating spider-silk-like microfibers. The structure of jet templates can be precisely adjusted by simply changing the flow rates to tailor the structures of the resultant spider-silk-like microfibers. The microfibers can be well manipulated by external magnetic fields for controllably moving, and patterning and assembling into different 2D and 3D structures. Moreover, the dehydrated spider-silk-like microfibers, with magnetic spindle-knots for collecting water drops, can be controllably assembled into spider-web-like structures for excellent water collection. These spider-silk-like microfibers are promising as functional building blocks for engineering complex 3D scaffolds for water collection, cell culture, and tissue engineering.

KEYWORDS: *biomimetic microfibers, microfluidics, template synthesis, magnetic assembly, water collection*

INTRODUCTION

Ordered arrangement and assembly of microstructures, such as natural spider silk microfibers, cactus spines, and hydrophobic/hydrophilic surfaces of beetle wings, are crucial to achieve advanced physical−chemical and biological functions.[1−4] Especially, spider silks are natural microfibers with wet-rebuilt periodic spindle-knots for capturing water from humid air,[1,5,6] and orderly assembly of these spider silks enables construction of webs with enhanced strength and ability for prey catching and water collection.[7−16] Inspired by the spider silks, a variety of functional microfibers have been developed from polymers such as poly(methyl methacrylate), azobenzene, poly(*N*-isopropylacrylamide), alginate, and proteins in recent years.[17−21] Incorporation of polymer spindle-knots into these microfibers allows construction of spider-silk-like structures for collection of water at their knot parts, exhibiting great potential in applications such as water collection, smart catalysis, filtration, and sensing.[22] However, although each single microfiber shows advanced functions in myriad fields, controllable 3D assembly of the microfibers for achieving integrated overall performance still remains challenging. Therefore, development of spider-silk-like microfibers with controllable assembling behaviors is highly desired for constructing complex assembled structures for enhanced applications such as water collection, cell culturing, and tissue engineering.

Microfibers can be easily produced by various methods such as electrospinning,[23,24] wet spinning,[25,26] and microfluidic approaches.[27−37] Typically, microfibers with separated spindle-knots can be achieved by dip-coating of commercial microfibers into polymer solutions.[1,20,38] Thus, polymer solution drops can form along the microfiber due to the Rayleigh instability, and then spindle-knots are generated after evaporating the solvent of the polymer solution drops. Alternatively, such spindle-knotted microfibers can also be obtained by electrodynamic technology.[39] By using a sprayable outer fluid with low viscosity and a spinnable inner fluid with high viscosity in a coaxial jetting process, hydrophilic spindle-knots are successfully imprinted on a hydrophobic string, resulting in spindle-knotted microfibers. Microfibers with improved control of their spindle-knot formation can be fabricated by a microfluidic technique. Such a technique provides excellent manipulation on microflow jets,[17,29,30,40−42] showing great potential for manufacturing microfibers with controllable separated external or internal knots.[17,43−47] By using a microfluidic chip combined with a digital fluid controller and pneumatic valves, spider-silk-like calcium alginate (CaAlg) microfibers with controllable external

Received: June 9, 2015
Accepted: July 20, 2015
Published: July 20, 2015

DOI: 10.1021/acsami.5b05075
ACS Appl. Mater. Interfaces 2015, 7, 17471−17481

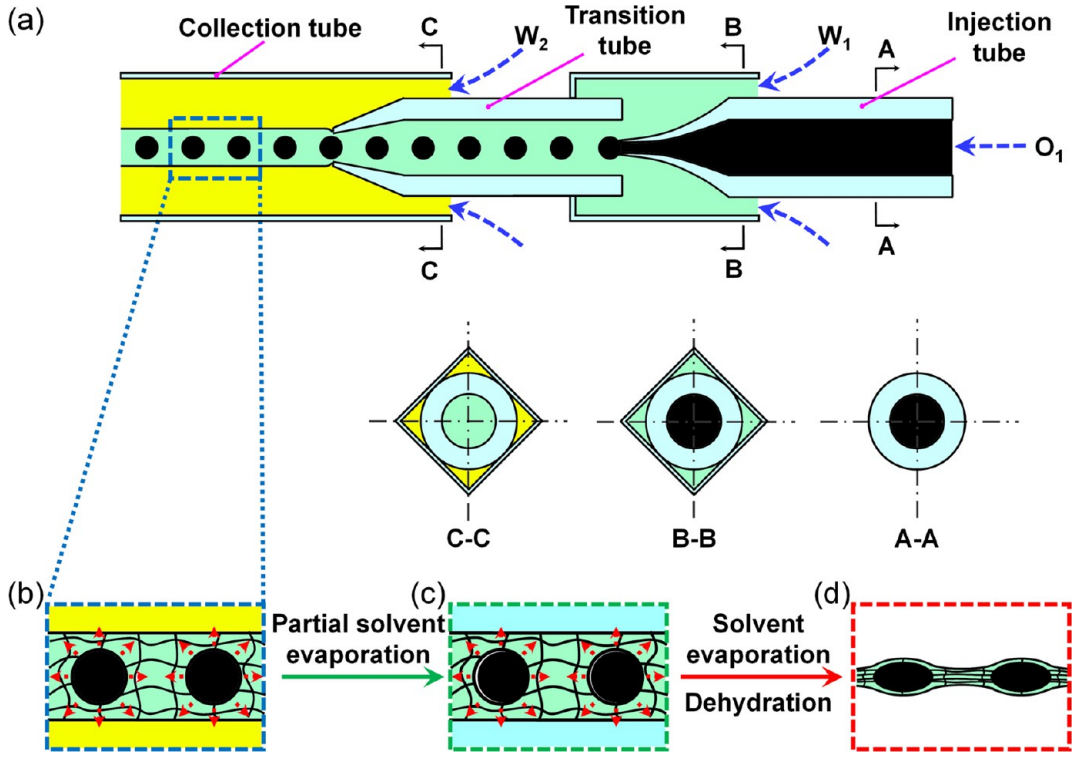

Figure 1. Schematic illustration of the microfluidic fabrication of CaAlg microfibers with controllable magnetic spindle-knots. (a) Microfluidic device for generation of jet templates for fabricating CaAlg microfibers. (b, c) Solvent evaporation process for constructing the magnetic knots. (d) Solvent evaporation combined with drying process for fabricating CaAlg microfibers with magnetic spindle-knots.

spindle-knots are developed from jet templates for water collection.[17] However, these microfibers remain difficult to be flexibly patterned and assembled, and the pneumatic-valve-based introduction of the spindle-knots remains troublesome and requires complex equipment. With combination of microfluidic jets and drops, cylinder-shaped microfibers with separate internal oil drops as knots can be generated from drop-containing jet templates for multiencapsulation.[43−47] For example, CaAlg microfibers with magnetic oil cores, and CaAlg microfibers with oil cores containing magnetic CaAlg microgels have been developed for encapsulation and release;[45] however, their liquid cores remain unstable for long-term use. Therefore, simple fabrication of robust spider-silk-like microfibers for flexible construction of controllable 3D assembling structures for enhanced performance still remains unavailable and challenging.

Here we report on a simple and flexible microfluidic strategy for controllable fabrication of spider-silk-like microfibers with tunable magnetic solid spindle-knots from biocompatible CaAlg for controlled 3D assembly and water collection. Liquid jet templates, with volatile oil drops containing magnetic Fe_3O_4 nanoparticles, are generated from microfluidics as templates for fabricating the spider-silk-like CaAlg microfibers via chemical cross-linking, solvent evaporating, and drying. The solvent evaporating and drying processes also lead to precipitation of the magnetic Fe_3O_4 nanoparticles to form spindle-knots in the dehydrated microfiber. The size of the microfiber and spindle-knots, as well as the distance between spindle-knots, can be precisely manipulated by simply changing the flow rates. The controllable magnetic spindle-knots in the microfibers enable excellent magnetic-manipulation of the microfibers for constructing controllably assembled structures for water collection. We demonstrate the magnetic-manipulation by manipulating hydrated CaAlg microfibers under different 2D and 3D setups of magnetic fields for controllable moving, patterning, and assembling. Moreover, the excellent water collection ability is demonstrated by assembling dehydrated CaAlg microfibers into spider-web-like structures for collecting water drops at their magnetic spindle-knots. These spider-silk-like CaAlg microfibers are promising as building blocks for constructing complex 3D scaffolds for water collection, cell culture, and tissue engineering. This approach provides a facile strategy for fabrication of spider-silk-like microfibers with controllable magnetic spindle-knots for controlled 3D assembly and water collection.

EXPERIMENTAL SECTION

Materials. Sodium alginate (NaAlg) was provided by Tianjin Kermel Chemical Reagents. Calcium chloride anhydrous ($CaCl_2$), *n*-hexane, and *N*-butyl acetate were purchased from Chengdu Kelong Chemical Reagents. Hydroxyethyl cellulose (HEC, 3400−5000 mPa·s, 25 °C) was obtained from Aladdin Industrial Corporation. Disperse Red was purchased from Jialong Dyeing. Ferrofluid was prepared by dispersing the oleic-acid-modified magnetic nanoparticles (OA-MNPs) in 15 mL of *n*-hexane, according to our previously reported procedures.[48] The OA-MNPs show an average diameter of ∼12 nm and saturation magnetization (M_s) of 52.26 emu g^{-1} (see Figures S1 and S2 for the TEM image and magnetization hysteresis loop of the OA-MNPs), and the content in ferrofluid is ∼92.65 mg mL^{-1} (∼12.8 wt %).

Microfluidic Fabrication of CaAlg Microfibers with Magnetic Spindle-Knots. A capillary microfluidic device used for microfiber fabrication was prepared according to our previous work (Figure 1a).[44] Illustrations A−A, B−B, and C−C in Figure 1a are cross section images of the capillary

DOI: 10.1021/acsami.5b05075
ACS Appl. Mater. Interfaces 2015, 7, 17471−17481

microfluidic device in relevant positions, which clearly show the assembly of the square capillary tubes and cylindrical tubes in the device. The inner diameters of the front-ends of the injection tube and the transition tube are 80 and 200 μm, respectively.

Jet templates with magnetic oil cores were prepared from the microfluidic device for fabrication of CaAlg microfibers with magnetic spindle-knots. Briefly, an oil mixture of ferrofluid and *N*-butyl acetate, with volume ratio of 2:1, was used as the inner dispersed flow (O_1), an aqueous solution containing 5.0 wt % NaAlg was used as the middle jet flow (W_1), and an aqueous solution containing 1.0 wt % HEC and 5.0 wt % $CaCl_2$ was used as the outer continuous flow (W_2). The *N*-butyl acetate is used to make the inner dispersed flow easier to be sheared by the middle jet flow to form monodisperse magnetic oil drops, since pure ferrofluid is very stable and hard to be emulsified. At appropriate flow rates, the O_1 was first emulsified by the W_1 flow in the transition tube, to generate uniform magnetic O_1 drops. Then, the W_1 flow containing O_1 drops was shaped by W_2 flow into the jet, which contained a regular array of O_1 drops. Due to the rapid cross-linking reaction between NaAlg and Ca^{2+}, the Ca^{2+} in W_2 diffused into the W_1 jet and triggered the cross-linking of NaAlg in the W_1 jet, resulting in the production of CaAlg microfibers with knots of magnetic oil drops (Figure 1b). To avoid the clogging caused by cross-linked microfibers, the microfluidic device was vertically fixed, with the outlet of the collection tube immersed in an aqueous solution of 5.0 wt % $CaCl_2$. The collected microfibers with magnetic knots were quickly washed with water to remove excess Ca^{2+} and stored in pure water for further use. To further prepare CaAlg microfibers with magnetic spindle-knots, the newly prepared microfibers were exposed and dried in air for 12 h. This allows complete volatilization of the *n*-hexane and *N*-butyl acetate in the magnetic oil drops to produce solid magnetic cores, and it enables dehydration of the CaAlg microfiber shell to form a spindle shape around the magnetic core (Figure 1c–d).

Investigation of the Morphology of CaAlg Microfibers. The formation process of jet templates for the generation of hydrated microfibers with magnetic oil cores was monitored with an inverted optical microscope (IX71, Olympus) equipped with a high-speed digital camera (Miro3, Phantom, Vision Research). To make the edges of the resultant microfibers more visible and clear, 0.1 wt % Disperse Red was added to the W_1. The structures of the hydrated and dehydrated CaAlg microfibers were observed with a digital microscope (GE-5, Aigo) and a scanning electron microscope (SEM, G2 Pro, Phenom). The effects of flow rate of the outer continuous flow (Q_{W2}) on the diameter of the microfiber (D) and the distance between two magnetic knots (L) were quantitatively studied by analyzing the optical images of the generated microfibers under different Q_{W2}. The L was defined as the distance between the centers of two neighboring magnetic knots.

Mechanical Properties of CaAlg Microfibers. The mechanical properties of hydrated and dehydrated CaAlg microfibers were investigated with an electronic universal testing machine (EZLX1kN, Shimadzu) with a 10 N sensor. Hydrated CaAlg Microfibers with outer diameter of 350 μm, oil core diameter of 200 μm, and knot distance of 550 μm were used for the mechanical property measurement. As a control group, dehydrated microfibers made from the aforementioned hydrated microfibers were also used. The sample gauge length between two clamps was 20 mm, and the straining rate was 10 mm min^{-1}.

Investigation of Magnetic-Responsive Properties of Hydrated CaAlg Microfibers. To evaluate the manipulation property of the prepared microfibers by magnetic fields, the magnetic-guided motions of the microfibers were investigated by using 2D and 3D rotating magnetic fields. For the magnetic-guided motion under a 2D rotating magnetic field, a microfiber with length of 1 cm was used as sample, and placed in a Petri dish with pure water. A cuboid-shaped magnet (Size: 4 mm × 4 mm × 20 mm) with surface magnetic intensity of 1.2 T was positioned above the microfiber sample with a constant rotation speed of 7.5 rpm to guide the rotation movement of the microfiber. For the magnetic-guided motion under 3D rotating magnetic field, the experiment was performed in a transparent poly(methyl methacrylate) (PMMA) box (Height: 24 mm, Width: 24 mm, Length: 24 mm, Thickness: 2 mm) with pure water. A microfiber with length of 3 cm was used as sample. The two ends of the microfiber were respectively fixed on the centers of two opposite walls of the PMMA box, via attracting their magnetic knots on magnetic minipillars (Size: Φ 1 mm × 3 mm) that embedded in the wall. To achieve the 3D rotating magnetic field, a cylinder-shaped magnet (Size: Φ 20 mm × 8 mm) with surface magnetic intensity of 2.1 T that fixed on a L-shaped rotating rod, with a rotation movement of 7.5 rpm, was used to guide the microfiber rotation.

Investigation of Magnetic-Assisted Patterning of Hydrated and Dehydrated CaAlg Microfibers. The magnetic-assisted patterning behavior of hydrated and dehydrated microfibers was demonstrated by manually arranging the microfibers on a magnetic array under water into desired patterns, including letter patterns and multilayered matrix patterns. The magnetic array was constructed by embedding 6 × 5 magnetic minipillars (Size: Φ 1 mm × 3 mm) in a polydimethylsiloxane matrix with a thickness of 3 mm.

Investigation of Magnetic-Guided Assembly of Hydrated and Dehydrated CaAlg Microfibers. The magnetic-guided assembly behavior of the hydrated and dehydrated microfibers was performed in a water-containing holder incorporated with different numbers of magnetic minipillars (Size: Φ 1 mm × 3 mm) for constructing different 3D assembly patterns of microfibers.

Investigation of Water Collection Ability of Dehydrated CaAlg Microfibers. The water collection ability of the spider-silk-like dehydrated microfibers was investigated by respectively using a single microfiber and assembled microfibers with a spider-web-like pattern as samples. To study the water collection of a single microfiber, the dried microfiber with periodic magnetic spindle-knots was placed in the upflow of a water mist for water collection. The flow of water mist was generated by an ultrasonic humidifier (SC-X100J, Beijing YADU Science and Technology). The whole process was recorded with a digital microscope. To quantify the water collection ability, the average volume of water drops collected on a single spindle-knot at different collection times was measured from the snapshots of the recorded movie. Both spindle-knots and water drops were considered as ellipsoids, and the drop volume was calculated based on its actual height and width. Similarly, the water collection ability of hydrated microfibers that were used as the control group was also studied.

The water collection of the spider-web-like microfiber network was also investigated by the above-mentioned method.

DOI: 10.1021/acsami.5b05075
ACS Appl. Mater. Interfaces 2015, 7, 17471−17481

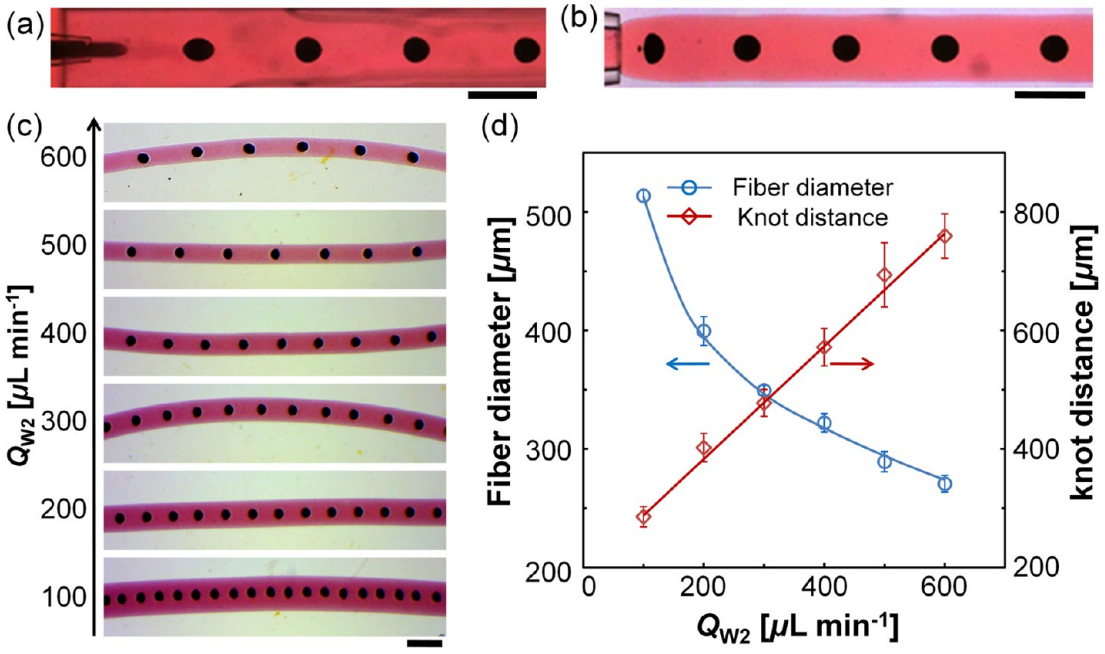

Figure 2. Flow-rate-dependent control of the structure of the jet templates and the resultant microfibers. (a, b) High-speed snapshots showing the generation processes of magnetic oil drops (a) and jet templates (b) in a microfluidic device. (c) Optical micrographs of the hydrated microfibers under different flow rate conditions. (d) Effects of Q_{W2} on the microfiber diameter (D) (blue line) and knot distance (L) (red line) of the hydrated microfibers. In (c) and (d), Q_{O1} and Q_{W1} are fixed at 20 μL min^{-1} and 200 μL min^{-1} respectively, and Q_{W2} is varied from 100 to 600 μL min^{-1}. The scale bars are 500 μm.

To construct the spider-web-like microfiber network, three dehydrated microfibers were assembled on a ring-shaped magnet, in which the microfibers were magnetically attracted by the middle magnetic knots at the center of the magnet with an angle of 60°.

RESULTS AND DISCUSSION

Fabrication of Microfibers with Controllable Magnetic Spindle-Knots. Jet templates with magnetic oil cores are generated for fabrication of CaAlg microfibers with magnetic oil cores (Figure 1a). Then, microfibers with magnetic spindle-knots are fabricated by dehydrating the CaAlg microfibers with magnetic oil cores (Figure 1b–d).

First, to generate the jet templates, the O_1 flow is emulsified into drops by W_1 flow in the transition tube of the microfluidic device (Figure 2a). After that, the W_1 flow that carries the O_1 drops is forced into a jet by shearing of W_2 (Figure 2b). The excellent microfluidic manipulation of the interfaces enables precise control of the jet structure as well as the resultant microfiber structure. The effects of flow rates on the morphology of this kind of peapod-like microfibers in a similar system and device have been systematically investigated in our previous study.[44] In this study, as an example, we investigate the effect of Q_{W2} on the morphology of the hydrated microfiber at fixed flow rates of O_1 (Q_{O1}, 20 μL min^{-1}) and W_1 (Q_{W1}, 200 μL min^{-1}). When Q_{W2} increases from 100 μL min^{-1} to 600 μL min^{-1}, the diameter of the microfiber (D) decreases from 513.7 to 270.6 μm (Figures 2c and 2d). Meanwhile, with such an increase of Q_{W2}, the distance between every two magnetic oil drops (L) increases, showing a linear relationship of $L = 0.953 \times Q_{W2} + 197.9$ (coefficient of determination $R^2 = 0.994$). Such a distance control defines the distribution of magnetic knots within the resultant dehydrated microfibers, which is important for the magnetic patterning and assembling behaviors of the microfibers. Moreover, in our experiments, when Q_{W1} and Q_{W2} are increased, the shape of the magnetic cores still remains spherical. All the results demonstrate the excellent control of the microfluidic approach for flexibly fabricating microfibers with controllable magnetic spindle-knots.

Cross-linking of the controllable jet templates produces hydrated CaAlg microfiber with magnetic oil cores, which can be continuously produced and collected by a spinning procedure (Figure 3a). In our experiments, under stable microfluidic spinning conditions, the microfiber can be produced continuously until one of the three flows runs out. The prepared CaAlg microfibers exhibit uniform structures similar to the jet templates, with monodisperse magnetic oil cores uniformly distributed in the CaAlg matrix of the microfiber (Figure 3b). After microfiber cross-linking, the oil cores become smaller than the cavity compartment of the microfiber (Figure 3c), due to the gradual evaporation of *n*-hexane and *N*-butyl acetate in the magnetic oil cores. Such an evaporation process lasts for a long time when the microfibers are immersed in water. To fabricate dehydrated microfibers with magnetic spindle-knots, the hydrated CaAlg microfibers are exposed in air; thus, the evaporation process can be significantly accelerated and accomplished after 12 h of drying. The effects of different drying rates on the morphology of the dehydrated CaAlg microfibers are studied for optimizing the drying conditions (see the Supporting Information for experimental details and Figure S3 for the results). The resultant dehydrated microfibers exhibit unique spider-silk-like structure, with uniform magnetic spindle-knots periodically distributed along the microfiber (Figure 3d). The spider-silk-like structures are caused by the shrinkage of the microfiber shell during drying, which deforms the spherical magnetic oil cores into solid magnetic cores with spindle shape. Moreover, when the distance between two magnetic cores is very short,

DOI: 10.1021/acsami.5b05075
ACS Appl. Mater. Interfaces 2015, 7, 17471–17481

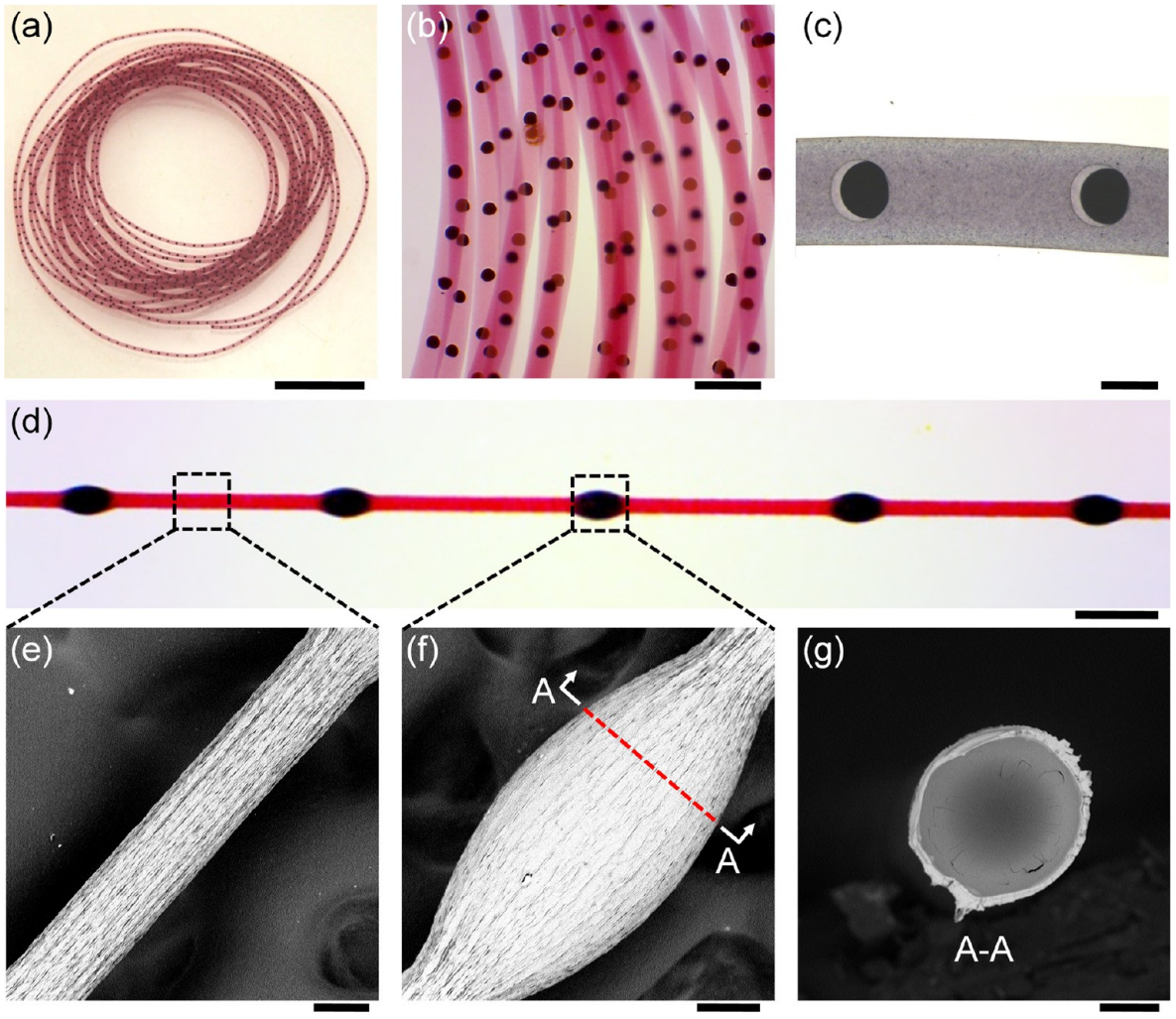

Figure 3. Morphological characterization of the hydrated microfibers and dehydrated microfibers with magnetic spindle-knots. (a–c) Digital photo (a), optical micrograph (b), and magnified optical micrograph (c) of the hydrated microfibers with magnetic oil cores. (d) Optical micrograph of the dehydrated microfibers with periodically arrayed magnetic spindle-knots. (e–g) SEM images of the outer surface of the joint part (e), and the outer surface (f) and cross section (g) of the spindle-knot of dehydrated microfibers. The scale bars are 1 cm in part a, 1 mm in part b, 200 μm in part c, 500 μm in part d, and 50 μm in parts e, f, and g.

only spindle-knots can be obtained along the dehydrated microfiber, without the presence of the joint parts (Figure S4). Specifically, to obtain the spider-silk-like microfiber (Figure 3d), the hydrated microfibers (Figure S5) shrink from ~361 μm to ~97 μm in diameter and shrink by ~14% in length during the dehydration process. As a result, the spherical oil cores are deformed and shrink from ~206 μm to ~168 μm in height and extend from ~206 μm to ~303 μm in width, leading to formation of spindle-shaped magnetic cores. Thus, spindle-shaped solid magnetic cores are obtained after evaporating the solvent of the oil cores to produce spider-silk-like microfibers. The diameters of the joint parts (Figure 3e) and spindle-knots (Figure 3f) in the dehydrated microfibers are 97 and 168 μm, respectively. The CaAlg shell of the spindle-knot compartment in the dehydrated microfiber is ~10 μm, as seen from the SEM image of the cross section (Figure 3g). The dehydrated CaAlg microfibers show improved stiffness and strength compared to the hydrated ones (see Figure S6 and Table S1 in the Supporting Information for details). Their stress–strain curves show that the fracture strains of the hydrated and dehydrated microfibers are ~144.79% and ~25.28%, respectively. The tensile strengths of the hydrated and dehydrated microfibers are 0.82 ± 0.03 MPa and 15.39 ± 0.40 MPa, respectively. The Young's moduli of the hydrated and dehydrated CaAlg microfibers are 0.70 ± 0.03 MPa and 533.57 ± 59.90 MPa, respectively. Their mechanic properties indicate that the stiffness and strength of the microfibers are significantly enhanced after dehydration. All the results show the great power of our strategy for preparing CaAlg microfibers with controllable magnetic spindle-knots.

Magnetic-Responsive Properties of Hydrated CaAlg Microfibers. The magnetic knots of hydrated CaAlg microfibers allow wireless manipulation of the microfibers with external 2D and 3D rotating magnetic fields. Under a 2D rotating magnetic field, the microfiber placed in a Petri dish can correspondingly rotate with the rotation of an external magnet (Figure 4a and Movie S1). The rotation process results from the interactions between the magnetic field and the magnetized superparamagnetic Fe_3O_4 nanoparticles contained in the magnetic knots. Under constant magnetic field, each magnetic knot tends to establish an individual magnetic dipole aligned to the applied field, which provides a net torque to make the microfiber rotate until the direction of the microfibers is parallel with the rotating magnet bar.[49] Moreover, we further

DOI: 10.1021/acsami.5b05075
ACS Appl. Mater. Interfaces 2015, 7, 17471–17481

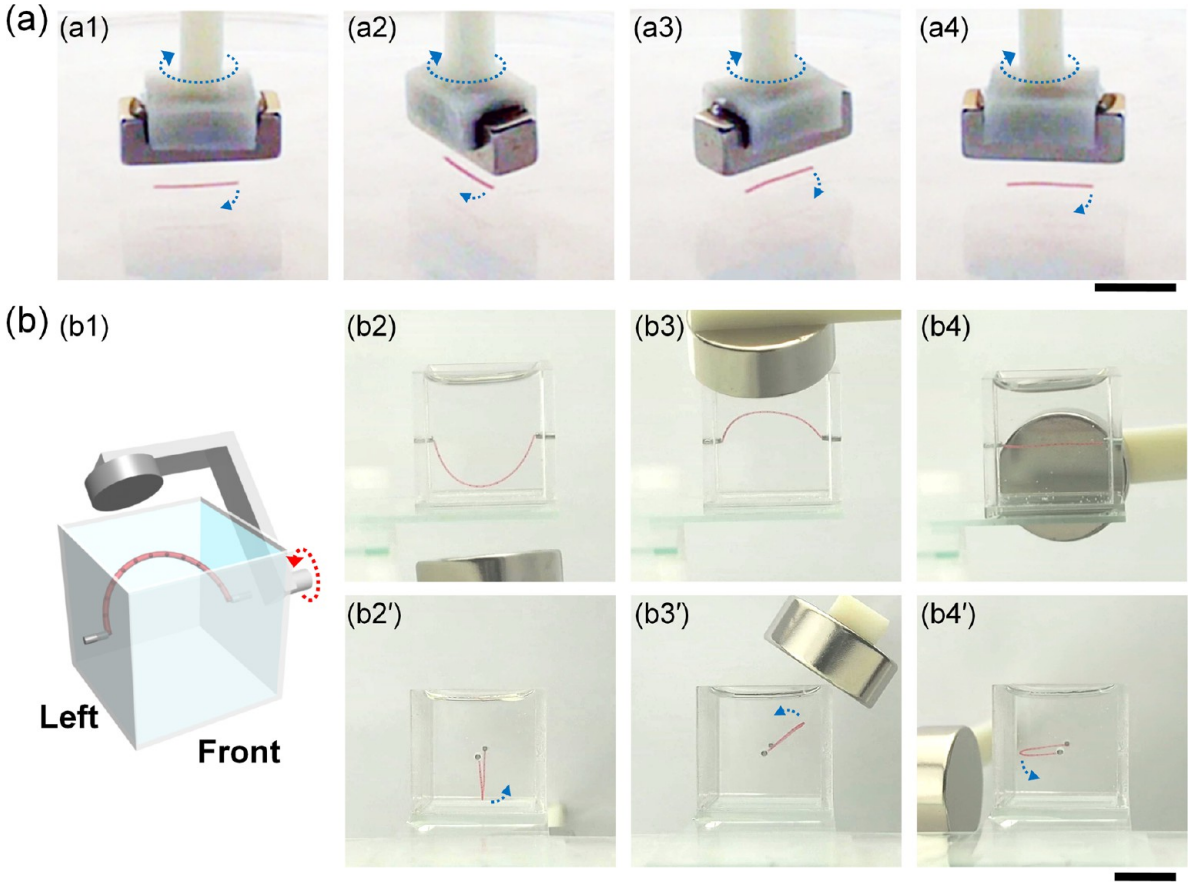

Figure 4. Magnetic manipulation of hydrated microfibers. (a) Digital photos showing the magnetic-guided 2D rotation of the microfiber. (b) Schematic illustration (b1) and snapshots (b2−b4 and b2′−b4′) showing the experiments for magnetic-guided 3D rotation of the microfiber. Snapshots (b2−b4) and (b2′−b4′) are respectively observed from the front view and left view. The scale bars are 1 cm.

demonstrate the 3D magnetic manipulation of a curved microfiber with two endmost magnetic knots fixed on magnetic minipillars embedded in the wall of a container (Figure 4b1 and Movie S2). With the two endmost magnetic knots fixed on the magnetic minipillars, the middle part of the microfiber can be attracted by the rotating magnet. As a result, the microfiber rotates correspondingly with the rotating magnet, with the two endmost magnetic knots as the rotating pivots. Such a 3D rotation movement of the curved microfiber is observed from the front (Figure 4b2−4) and left views (Figure 4b2′−4′), respectively, for better exhibiting the 3D synchronously rotation with the rotating magnet. The rotation axis of the microfiber is the same for both viewing cases. The results indicate the produced CaAlg microfibers have excellent magnetic-responsive properties for flexible arrangement and assembly. Moreover, the magnetic-responsive property of the microfibers mainly depends on their OA-MNPs content, which can be determined by employing the total volume of their magnetic oil cores and the microfiber mass based on the OA-MNPs content in the ferrofluid. Further improvement of the magnetic-responsive property can be obtained by increasing the OA-MNPs content. Such microfibers may show potential as mini-/micromixers for local stirring and mixing.

Magnetic-Guided Patterning and Assembling of Hydrated and Dehydrated CaAlg Microfibers. Incorporation of magnetic substances in materials can provide the materials with magnetic-guided patterning and assembling ability.[50−53] In this study, the magnetic responsive property of the hydrated CaAlg microfibers allows employment of different 2D and 3D setups of magnetic fields for flexibly patterning and assembling of these microfibers. We demonstrate this magnetic-guided patterning by using the CaAlg microfibers to construct different letter patterns on an array of magnetic minipillars (Figure 5a). The positions of all magnetic knots along the microfiber are manually adjusted and magnetically attracted on the tip of the magnetic minipillars. This enables patterning of the microfibers for spelling out the word “memhome”, the abbreviation for our lab (Figure 5a2−8). For the patterning, the microfibers show enough stiffness against the attractive force between two neighboring magnetic knots. Thus, bonding of two magnetic knots can only be achieved when the microfiber length between the two magnetic knots is long enough (Figure S7). Moreover, more complex textile-like structures can also be achieved by sequentially patterning multilayer microfiber networks, each consisting of 11 (Figure 5b1−2) or 22 (Figure 5b3−4) cross-aligned microfibers. Similar magnetic-guided patterning and assembling behaviors can be achieved for the dehydrated CaAlg microfibers (Figures S8 and S9).

The magnetic-guided assembling of the hydrated CaAlg microfibers is shown by using three different 3D magnetic fields that are respectively constructed by using magnetic minipillars with numbers of n = 1, 2, and 4. The hydrated microfibers are manually adjusted and magnetically attracted on the tip of magnetic minipillars. The schematic diagrams of the setups of 1, 2, and 4 magnetic minipillars for controllable microfiber

DOI: 10.1021/acsami.5b05075
ACS Appl. Mater. Interfaces 2015, 7, 17471−17481

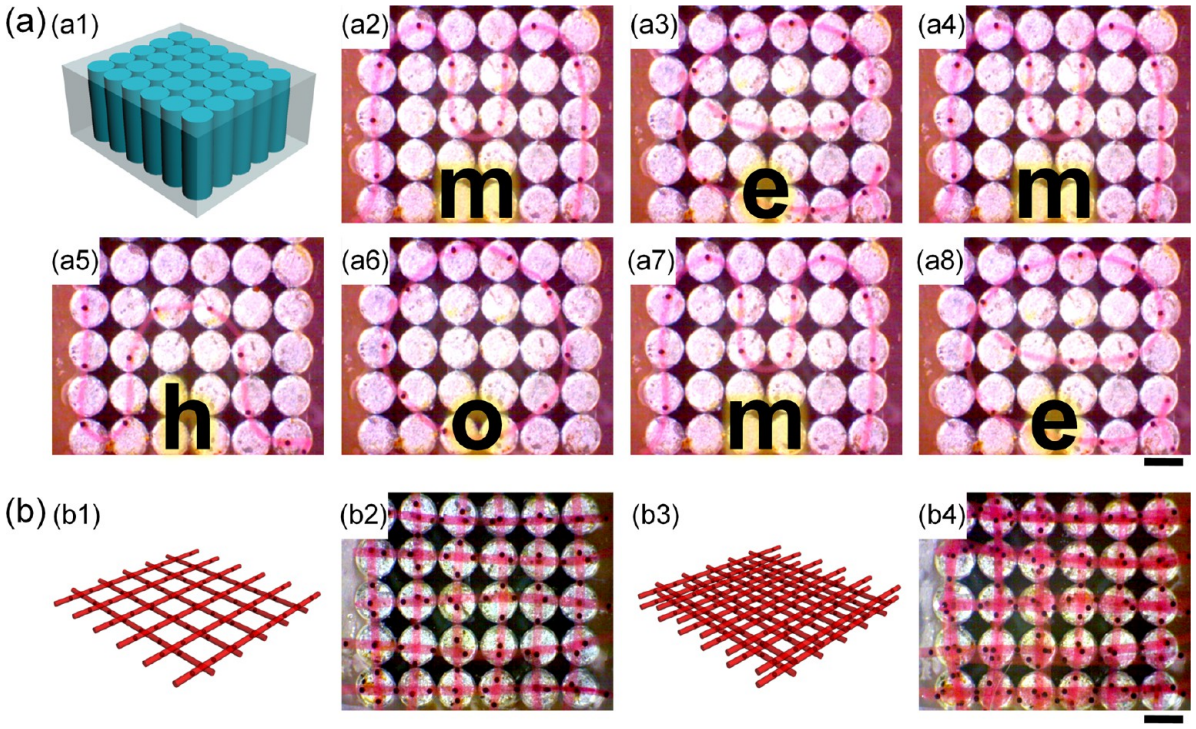

Figure 5. Magnetic patterning of the hydrated microfibers. (a) Schematic illustration (a1) of the magnetic arrays for microfiber patterning, and optical micrographs (a2−a8) showing different 2D letter patterns ("memhome") arranged from the hydrated microfibers. (b) Schematic illustrations and optical micrographs of the 3D textile-like patterns constructed from 11 (b1−b2) and 22 (b3−b4) microfibers. The scale bars are 1 mm.

assembly are shown in Figures 6a1, 6b1, and 6c1, respectively. For n = 1, the microfibers, each with one end attracted on the magnetic minipillar, are assembled into a semiradial geometry, because their free ends are oriented by a similar semiradial magnetic field distribution near the magnetic minipillar (Figure 6a2−a3).[54,55] For n = 2, the microfibers, each with both ends attracted by the magnetic minipillars, are parallelly assembled into a columnar shape (Figure 6b2−b3), while the microfibers are assembled into a cross-shaped structure for n = 4 (Figure 6c2−c3). The magnetic-guided patterning and assembling only requires the existence of magnetic knots where the magnetic minipillars are located. Thus, since the distance between two magnetic knots can be flexibly defined by adjusting flow rates, the maximum limit distance between two magnetic knots mainly depends on the setup styles of the magnetic minipillars. All the results show the excellent performance of these microfibers for controllable and flexible patterning and assembling under well-designed magnetic fields.

Water Collection of Dehydrated CaAlg Microfibers with Magnetic Spindle-Knots. The excellent magnetic-guided assembling behavior of the microfibers enables fabrication of artificial spider-web-like networks for water collection. First, we investigate the water collection ability of a single dehydrated CaAlg microfiber by slightly obliquely placing the microfiber in an upflow of water mist (Figure 7a and Movie S3). At the beginning, the hydrophilic CaAlg microfiber allows adsorption of tiny water drops from the water mist into the cross-linked matrix to give slight swelling (Figure 7a1). Then, as the water condensation continues, larger water drops are randomly formed at the spindle-knot part or joint part along the microfiber. Interestingly, although the dehydrated microfiber is placed obliquely for water collection, the water drops formed in the lower joint part can overcome their own gravity and move directionally to the neighboring upper spindle-knot, and then coalesce with other water drops at the spindle-knot for water collection (Figure 7a2−6). Similar water collection behaviors on the spindle-knots can be observed for horizontally placed dehydrated CaAlg microfibers (Figure S10). By contrast, when applying the hydrated microfibers to the water mist, water drops collected on the CaAlg matrix can randomly move along the microfiber (Figure S11); thus, their magnetic knots cannot be used for water collection. To evaluate the water collection ability of the dehydrated microfibers, the average volume of water drops collected on a single spindle-knot of the dehydrated microfibers as a function of collection time is shown in Figure 7b. After a short collection time (t = 3 s), water drops (~346 μm in height, ~615 μm in width) with volume of 34.60 nL, which is ~9 times of that of the spindle-knot (~162 μm in height, ~292 μm in width, and ~3.99 nL in volume), can be collected on the spindle-knot. At 19 s, water drops with volume of ~365 nL can be collected, which is ~92 times that of the spindle-knot. The results show the excellent water collection ability of the dehydrated microfibers. Moreover, since the spindle-knot size can be easily increased via changing the microfluidic flow rates, further enhancement of the water collection ability can be simply achieved by employing larger spindle-knots, which has been clarified by other studies previously.[56]

Generally, the driving force of water drops toward the spindle-knots part is mainly caused by three factors: (1) chemical force induced by the surface wettability difference between the spindle-knot and the joint part, (2) hysteresis resistance due to water contact angle hysteresis, and (3) the Laplace force induced by the curvature gradient from the joint part to the spindle-knot.[20] Since the joints and spindle-knots in our microfibers show different surface structures (Figure S12), we hypothesize that all three forces, including the chemical

DOI: 10.1021/acsami.5b05075
ACS Appl. Mater. Interfaces 2015, 7, 17471−17481

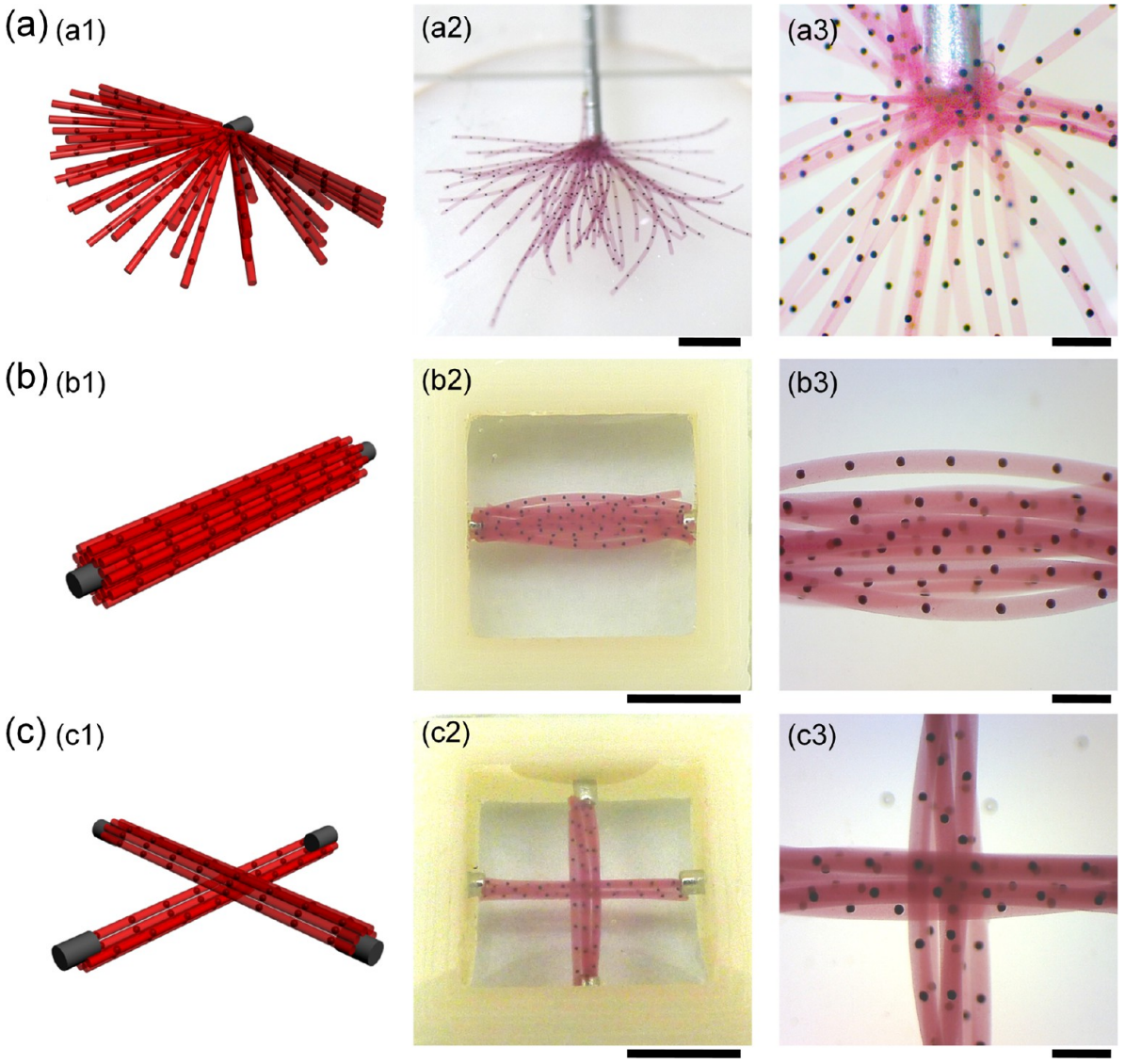

Figure 6. Magnetic-guided assembly of the hydrated microfibers. Schematic illustrations (a1−c1), digital photos (a2−c2), and optical micrographs (a3−c3) of the 3D assembly structures of hydrated microfibers guided by one (a), two (b), and four (c) magnetic minipillars. The scale bars are 5 mm in a2, b2, and c2, and 1 mm in a3, b3, and c3.

force, hysteresis resistance, and Laplace force, are involved in the driving process of water drops for water collection.

Based on the water collection ability of the spider-silk-like microfibers, we further assemble these microfibers on a circle-shaped magnet to construct an artificial spider web (Figure 7c1). The two ends of each microfiber are fixed on the circle-shaped magnet, and the three magnetized spindle-knots in the center of the microfibers are attracted to each other, resulting in a stable spider-web-like structure (Figures 7c1 and 7c2). When placing this artificial spider web in the upflow of a water mist, large water drops are collected at each of the spindle-knots in the artificial spider web, exhibiting excellent water collection ability (Figure 7c3). The results demonstrate the potential of our microfibers for controllable and flexible construction of complex assembling structures for water collection. Moreover, since the uniform spindle-knots along the microfibers possess the same water collection ability, the water collection efficiency of the microfiber patterning can be enhanced by increasing the number of spindle-knots contained in the patterning.

CONCLUSIONS

In summary, a simple and flexible strategy has been developed for continuous fabrication of spider-silk-like CaAlg microfibers with tunable magnetic spindle-knots from microfluidic jet templates for controlled 3D assembly and water collection. The excellent flow-rate-dependent manipulation of the structure of the jet templates, together with the *in situ* cross-linking, solvent evaporating, and drying process, enables facile and flexible adjustment of the resultant microfiber structures. Under elaborate setups of different magnetic fields, the microfibers can be well manipulated for controllably moving, patterning, and assembling. Based on the water collection ability of a single dehydrated microfiber with periodic magnetic spindle-knots, the microfibers can be controllably assembled into spider-web-like structures for excellent water collection. This novel type of spider-silk-like CaAlg microfibers creates opportunities for controllably constructing scaffolds with complex 3D networks for cell culture and tissue engineering; meanwhile, such scaffolds can also be simply dissembled by removing the magnetic field to harvest the cultured functional cells and

DOI: 10.1021/acsami.5b05075
ACS Appl. Mater. Interfaces 2015, 7, 17471−17481

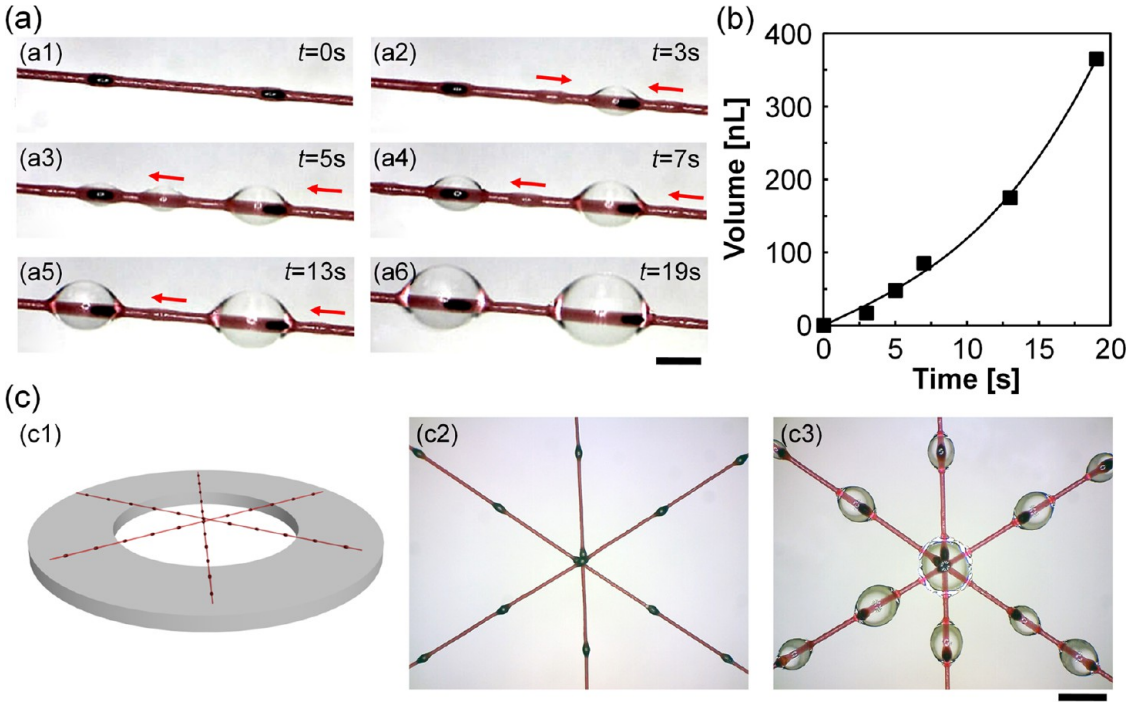

Figure 7. Dehydrated microfibers with magnetic spindle-knots and their assembly of spider-web-like structure for water collection. (a) Optical images showing the water collection process on the dehydrated microfiber with magnetic spindle-knots. (b) Water collection volume on a single spindle-knot as a function of collection time. (c) Schematic illustration showing the assembly of dehydrated microfiber for constructing spider-web-like structures (c1), and optical images showing the spider-web-like structures before (c2) and after (c3) the water collection. The scale bars are 500 μm in part a and 1 mm in part c.

tissues, and their bioactive products, and then reassembled for repeated use. Moreover, the spider-silk-like microfiber structures provide potential candidates for fabricating advanced microfibers by using stimuli-responsive or other functional materials to construct the spindle-knots for applications such as controlled liquid transportation,[18,19] drug release,[45] and coding.[43] Therefore, these spider-silk-like CaAlg microfibers show great potential for controllable assembly of complex 3D scaffolds for water collection, cell culture, and tissue engineering, and for developing novel functional microfibers.

■ ASSOCIATED CONTENT

Supporting Information

Experimental details and results about the drying rate optimization for dehydration, TEM image and magnetic property of OA-MNPs, optical micrographs of hydrated microfibers and dehydrated microfibers without joint parts, mechanical properties of the microfibers, magnetic attractive behavior of two magnetic knots, patterning and assembling of dehydrated microfibers, water collection of horizontally placed hydrated and dehydrated microfibers, and magnified SEM of the surface structures of the joint part and spindle-knot part. The Supporting Information is available free of charge on the ACS Publications website at DOI: 10.1021/acsami.5b05075.

■ AUTHOR INFORMATION

Corresponding Authors

*E-mail: wangwei512@scu.edu.cn (W. Wang).
*E-mail: chuly@scu.edu.cn (L.-Y. Chu).

Notes

The authors declare no competing financial interest.

■ ACKNOWLEDGMENTS

The authors gratefully acknowledge support from the National Natural Science Foundation of China (21136006, 21306117, 81321002), and State Key Laboratory of Polymer Materials Engineering (sklpme2014-1-01).

■ REFERENCES

(1) Zheng, Y. M.; Bai, H.; Huang, Z. B.; Tian, X. L.; Nie, F. Q.; Zhao, Y.; Zhai, J.; Jiang, L. Directional Water Collection on Wetted Spider Silk. *Nature* **2010**, *463*, 640−643.
(2) Parker, A. R.; Lawrence, C. R. Water Capture by a Desert Beetle. *Nature* **2001**, *414*, 33−34.
(3) Cao, M. Y.; Ju, J.; Li, K.; Dou, S. X.; Liu, K. S.; Jiang, L. Facile and Large-Scale Fabrication of a Cactus-Inspired Continuous Fog Collector. *Adv. Funct. Mater.* **2014**, *24*, 3235−3240.
(4) Ozden, S.; Ge, L. H.; Narayanan, T. N.; Hart, A. H. C.; Yang, H.; Sridhar, S.; Vajtai, R.; Ajayan, P. M. Anisotropically Functionalized Carbon Nanotube Array Based Hygroscopic Scaffolds. *ACS Appl. Mater. Interfaces* **2014**, *6*, 10608−10613.
(5) Hancock, M. J.; Sekeroglu, K.; Demirel, M. C. Bioinspired Directional Surfaces for Adhesion, Wetting, and Transport. *Adv. Funct. Mater.* **2012**, *22*, 2223−2234.
(6) Zhao, N.; Wang, Z.; Cai, C.; Shen, H.; Liang, F. Y.; Wang, D.; Wang, C. Y.; Zhu, T.; Guo, J.; Wang, Y. X.; Liu, X. F.; Duan, C. T.; Wang, H.; Mao, Y. Z.; Jia, X.; Dong, H. X.; Zhang, X. L.; Xu, J. Bioinspired Materials: From Low to High Dimensional Structure. *Adv. Mater.* **2014**, *26*, 6994−7017.
(7) Walter, A.; Cadenhead, N.; Lee, V. S. W.; Dove, C.; Milley, E.; Elgar, M. A. Water as an Essential Resource: Orb Web Spiders Cannot Balance Their Water Budget by Prey Alone. *Ethology* **2012**, *118*, 534−542.
(8) Watanabe, T. Effects of Web Design on the Prey Capture Efficiency of the Uloborid Spider Octonoba Sybotides under Abundant and Limited Prey Conditions. *Zool. Sci.* **2001**, *18*, 585−590.

DOI: 10.1021/acsami.5b05075
ACS Appl. Mater. Interfaces 2015, 7, 17471−17481

(9) Eberhard, W. G. Function and Phylogeny of Spider Webs. *Annu. Rev. Ecol. Syst.* **1990**, *21*, 341−372.
(10) Eisoldt, L.; Smith, A.; Scheibel, T. Decoding the Secrets of Spider Silk. *Mater. Today* **2011**, *14*, 80−86.
(11) Blackledge, T. A.; Scharff, N.; Coddington, J. A.; Szüts, T.; Wenzel, J. W.; Hayashi, C. Y.; Agnarsson, I. Reconstructing Web Evolution and Spider Diversification in the Molecular Era. *Proc. Natl. Acad. Sci. U. S. A.* **2009**, *106*, 5229−5234.
(12) Venner, S.; Casas, J. Spider Webs Designed for Rare but Life-Saving Catches. *Proc. R. Soc. London, Ser. B* **2005**, *272*, 1587−1592.
(13) Peñalver, E.; Grimaldi, D. A.; Delclòs, X. Early Cretaceous Spider Web with Its Prey. *Science* **2006**, *312*, 1761−1761.
(14) Cranford, S. W.; Tarakanova, A.; Pugno, N. M.; Buehler, M. J. Nonlinear Material Behaviour of Spider Silk Yields Robust Webs. *Nature* **2012**, *482*, 72−76.
(15) Qin, Z.; Compton, B. G.; Lewis, J. A.; Buehler, M. J. Structural Optimization of 3D-Printed Synthetic Spider Webs for High Strength. *Nat. Commun.* **2015**, *6*, 7038.
(16) Gosline, J. M.; Guerette, P. A.; Ortlepp, C. S.; Savage, K. N. The Mechanical Design of Spider Silks: From Fibroin Sequence to Mechanical Function. *J. Exp. Biol.* **1999**, *202*, 3295−3303.
(17) Kang, E.; Jeong, G. S.; Choi, Y. Y.; Lee, K. H.; Khademhosseini, A.; Lee, S. H. Digitally Tunable Physicochemical Coding of Material Composition and Topography in Continuous Microfibres. *Nat. Mater.* **2011**, *10*, 877−883.
(18) Hou, Y. P.; Gao, L. C.; Feng, S. L.; Chen, Y.; Xue, Y.; Jiang, L.; Zheng, Y. M. Temperature-Triggered Directional Motion of Tiny Water Droplets on Bioinspired Fibers in Humidity. *Chem. Commun.* **2013**, *49*, 5253−5255.
(19) Feng, S. L.; Hou, Y. P.; Xue, Y.; Gao, L. C.; Jiang, L.; Zheng, Y. M. Photo-Controlled Water Gathering on Bio-Inspired Fibers. *Soft Matter* **2013**, *9*, 9294−9297.
(20) Bai, H.; Tian, X. L.; Zheng, Y. M.; Ju, J.; Zhao, Y.; Jiang, L. Direction Controlled Driving of Tiny Water Drops on Bioinspired Artificial Spider Silks. *Adv. Mater.* **2010**, *22*, 5521−5525.
(21) Rising, A.; Johansson, J. Toward Spinning Artificial Spider Silk. *Nat. Chem. Biol.* **2015**, *11*, 309−315.
(22) Bai, H.; Ju, J.; Zheng, Y. M.; Jiang, L. Functional Fibers with Unique Wettability Inspired by Spider Silks. *Adv. Mater.* **2012**, *24*, 2786−2791.
(23) Kidoaki, S.; Kwon, I. K.; Matsuda, T. Mesoscopic Spatial Designs of Nano- and Microfiber Meshes for Tissue-Engineering Matrix and Scaffold Based on Newly Devised Multilayering and Mixing Electrospinning Techniques. *Biomaterials* **2005**, *26*, 37−46.
(24) Dror, Y.; Salalha, W.; Avrahami, R.; Zussman, E.; Yarin, A. L.; Dersch, R.; Greiner, A.; Wendorff, J. H. One-Step Production of Polymeric Microtubes by Co-Electrospinning. *Small* **2007**, *3*, 1064−1073.
(25) Grigoryev, A.; Sa, V.; Gopishetty, V.; Tokarev, I.; Kornev, K. G.; Minko, S. Wet-Spun Stimuli-Responsive Composite Fibers with Tunable Electrical Conductivity. *Adv. Funct. Mater.* **2013**, *23*, 5903−5909.
(26) Zhang, J. M.; Wang, L. N.; Zhu, M. F.; Wang, L. Y.; Xiao, N. N.; Kong, D. L. Wet-Spun Poly(Epsilon-Caprolactone) Microfiber Scaffolds for Oriented Growth and Infiltration of Smooth Muscle Cells. *Mater. Lett.* **2014**, *132*, 59−62.
(27) Jun, Y.; Kang, E.; Chae, S.; Lee, S. H. Microfluidic Spinning of Micro- and Nano-Scale Fibers for Tissue Engineering. *Lab Chip* **2014**, *14*, 2145−2160.
(28) Cheng, Y.; Zheng, F. Y.; Lu, J.; Shang, L. R.; Xie, Z. Y.; Zhao, Y. J.; Chen, Y. P.; Gu, Z. Z. Bioinspired Multicompartmental Microfibers from Microfluidics. *Adv. Mater.* **2014**, *26*, 5184−5190.
(29) Daniele, M. A.; North, S. H.; Naciri, J.; Howell, P. B.; Foulger, S. H.; Ligler, F. S.; Adams, A. A. Rapid and Continuous Hydrodynamically Controlled Fabrication of Biohybrid Microfibers. *Adv. Funct. Mater.* **2013**, *23*, 698−704.
(30) Jeong, W.; Kim, J.; Kim, S.; Lee, S.; Mensing, G.; Beebe, D. J. Hydrodynamic Microfabrication via "On the Fly" Photopolymerization of Microscale Fibers and Tubes. *Lab Chip* **2004**, *4*, 576−580.
(31) Choi, C. H.; Yi, H.; Hwang, S.; Weitz, D. A.; Lee, C. S. Microfluidic Fabrication of Complex-Shaped Microfibers by Liquid Template-Aided Multiphase Microflow. *Lab Chip* **2011**, *11*, 1477−1483.
(32) Oh, J.; Kim, K.; Won, S. W.; Cha, C.; Gaharwar, A. K.; Selimović, Š.; Bae, H.; Lee, K. H.; Lee, D. H.; Lee, S. H.; Khademhosseini, A. Microfluidic Fabrication of Cell Adhesive Chitosan Microtubes. *Biomed. Microdevices* **2013**, *15*, 465−472.
(33) Chae, S. K.; Kang, E.; Khademhosseini, A.; Lee, S. H. Micro/Nanometer-Scale Fiber with Highly Ordered Structures by Mimicking the Spinning Process of Silkworm. *Adv. Mater.* **2013**, *25*, 3071−3078.
(34) Yeh, C. H.; Lin, P. W.; Lin, Y. C. Chitosan Microfiber Fabrication Using a Microfluidic Chip and Its Application to Cell Cultures. *Microfluid. Nanofluid.* **2010**, *8*, 115−121.
(35) Marimuthu, M.; Kim, S.; An, J. Amphiphilic Triblock Copolymer and a Microfluidic Device for Porous Microfiber Fabrication. *Soft Matter* **2010**, *6*, 2200−2207.
(36) Lan, W. J.; Li, S. W.; Lu, Y. C.; Xu, J. H.; Luo, G. S. Controllable Preparation of Microscale Tubes with Multiphase Co-Laminar Flow in a Double Co-Axial Microdevice. *Lab Chip* **2009**, *9*, 3282−3288.
(37) Su, J.; Zheng, Y. Z.; Wu, H. K. Generation of Alginate Microfibers with a Roller-Assisted Microfluidic System. *Lab Chip* **2009**, *9*, 996−1001.
(38) Bai, H.; Sun, R. Z.; Ju, J.; Yao, X.; Zheng, Y. M.; Jiang, L. Large-Scale Fabrication of Bioinspired Fibers for Directional Water Collection. *Small* **2011**, *7*, 3429−3433.
(39) Tian, X. L.; Bai, H.; Zheng, Y. M.; Jiang, L. Bio-Inspired Heterostructured Bead-on-String Fibers that Respond to Environmental Wetting. *Adv. Funct. Mater.* **2011**, *21*, 1398−1402.
(40) Utada, A. S.; Chu, L. Y.; Fernandez-Nieves, A.; Link, D. R.; Holtze, C.; Weitz, D. A. Dripping, Jetting, Drops, and Wetting: The Magic of Microfluidics. *MRS Bull.* **2007**, *32*, 702−708.
(41) Wang, W.; Zhang, M. J.; Xie, R.; Ju, X. J.; Yang, C.; Mou, C. L.; Weitz, D. A.; Chu, L. Y. Hole-Shell Microparticles from Controllably Evolved Double Emulsions. *Angew. Chem., Int. Ed.* **2013**, *52*, 8084−8087.
(42) Onoe, H.; Okitsu, T.; Itou, A.; Kato-Negishi, M.; Gojo, R.; Kiriya, D.; Sato, K.; Miura, S.; Iwanaga, S.; Kuribayashi-Shigetomi, K.; Matsunaga, Y. T.; Shimoyama, Y.; Takeuchi, S. Metre-Long Cell-Laden Microfibres Exhibit Tissue Morphologies and Functions. *Nat. Mater.* **2013**, *12*, 584−590.
(43) Yu, Y.; Wen, H.; Ma, J. Y.; Lykkemark, S.; Xu, H.; Qin, J. H. Flexible Fabrication of Biomimetic Bamboo-Like Hybrid Microfibers. *Adv. Mater.* **2014**, *26*, 2494−2499.
(44) He, X. H.; Wang, W.; Deng, K.; Xie, R.; Ju, X. J.; Liu, Z.; Chu, L. Y. Microfluidic Fabrication of Chitosan Microfibers with Controllable Internals from Tubular to Peapod-Like Structures. *RSC Adv.* **2015**, *5*, 928−936.
(45) Um, E. J.; Nunes, J. K.; Pico, T.; Stone, H. A. Multicompartment Microfibers: Fabrication and Selective Dissolution of Composite Droplet-in-Fiber Structures. *J. Mater. Chem. B* **2014**, *2*, 7866−7871.
(46) Sun, T.; Hu, C. Z.; Nakajima, M.; Takeuchi, M.; Seki, M.; Yue, T.; Shi, Q.; Fukuda, T.; Huang, Q. On-Chip Fabrication and Magnetic Force Estimation of Peapod-Like Hybrid Microfibers Using a Microfluidic Device. *Microfluid. Nanofluid.* **2015**, *18*, 1177−1187.
(47) Ji, X. B.; Guo, S.; Zeng, C. F.; Wang, C. Q.; Zhang, L. X. Continuous Generation of Alginate Microfibers with Spindle-Knots by Using a Simple Microfluidic Device. *RSC Adv.* **2015**, *5*, 2517−2522.
(48) Liu, Y. M.; Wang, W.; Zheng, W. C.; Ju, X. J.; Xie, R.; Zerrouki, D.; Deng, N. N.; Chu, L. Y. Hydrogel-Based Microactuators with Remote-Controlled Locomotion and Fast Pb2+-Response for Micromanipulation. *ACS Appl. Mater. Interfaces* **2013**, *5*, 7219−7226.
(49) Jiang, K. Q.; Xue, C.; Arya, C. D.; Shao, C. R.; George, E. O.; DeVoe, D. L.; Raghavan, S. R. A New Approach to In-Situ "Micromanufacturing": Microfluidic Fabrication of Magnetic and Fluorescent Chains Using Chitosan Microparticles as Building Blocks. *Small* **2011**, *7*, 2470−2476.

DOI: 10.1021/acsami.5b05075
ACS Appl. Mater. Interfaces 2015, 7, 17471−17481

(50) Tasoglu, S.; Yu, C. H.; Gungordu, H. I.; Guven, S.; Vural, T.; Demirci, U. Guided and Magnetic Self-Assembly of Tunable Magnetoceptive Gels. *Nat. Commun.* **2014**, *5*, 4702.
(51) Xu, F.; Wu, C. A. M.; Rengarajan, V.; Finley, T. D.; Keles, H. O.; Sung, Y. R.; Li, B. Q.; Gurkan, U. A.; Demirci, U. Three-Dimensional Magnetic Assembly of Microscale Hydrogels. *Adv. Mater.* **2011**, *23*, 4254−4260.
(52) Mirica, K. A.; Ilievski, F.; Ellerbee, A. K.; Shevkoplyas, S. S.; Whitesides, G. M. Using Magnetic Levitation for Three Dimensional Self-Assembly. *Adv. Mater.* **2011**, *23*, 4134−4140.
(53) Liu, W.; Li, Y. Q.; Feng, S. Y.; Ning, J.; Wang, J. Y.; Gou, M. L.; Chen, H. J.; Xu, F.; Du, Y. A. Magnetically Controllable 3D Microtissues Based on Magnetic Microcryogels. *Lab Chip* **2014**, *14*, 2614−2625.
(54) Chang, C. H.; Tan, C. W.; Miao, J. M.; Barbastathis, G. Self-Assembled Ferrofluid Lithography: Patterning Micro and Nanostructures by Controlling Magnetic Nanoparticles. *Nanotechnology* **2009**, *20*, 495301.
(55) Lorenzo, D.; Fragouli, D.; Bertoni, G.; Innocenti, C.; Anyfantis, G. C.; Cozzoli, P. D.; Cingolani, R.; Athanassiou, A. Formation and Magnetic Manipulation of Periodically Aligned Microchains in Thin Plastic Membranes. *J. Appl. Phys.* **2012**, *112*, 083927.
(56) Bai, H.; Ju, J.; Sun, R. Z.; Chen, Y.; Zheng, Y. M.; Jiang, L. Controlled Fabrication and Water Collection Ability of Bioinspired Artificial Spider Silks. *Adv. Mater.* **2011**, *23*, 3708−3711.

DOI: 10.1021/acsami.5b05075
ACS Appl. Mater. Interfaces 2015, 7, 17471−17481